SUPPORTING INFORMATION

Highly durable catalyst system for hydrogen production from dimethyl ether

Robert Stöber,[a] Franziska Seidl,[a] Emanuel Hoffmann,[a] Peter Wasserscheid, [a,b,c] and Patrick Schühle *[a]

[1] *Lehrstuhl für Chemische Reaktionstechnik, Friedrich-Alexander-Universität Erlangen-Nürnberg, Egerlandstr. 3, 91058 Erlangen, Germany*
[2] *Forschungszentrum Jülich, Helmholtz-Institute Erlangen-Nürnberg for Renewable Energy (IEK 11), Egerlandstr. 3, 91058 Erlangen, Germany*
[3] *Forschungszentrum Jülich, Institute for a Sustainable Hydrogen Economy, Am Brainergy Park 4, 52428 Jülich, Germany*
* *Patrick.Schuehle@fau.de*

Synthesis of PdZn/Al_2O_3:

For the wetness impregnation of PdZn with a molar ratio of Pd:Zn 1:1 on Al_2O_3, Aluminium oxide (thermo scientific, γ-phase, bimodal pore size distribution, high surface area, 1/8" catalyst support), zinc nitrate hexahydrate (Alfa Aesar, 99*%* metals basis) and ammonium hexachloropalladate (thermo scientific, 99.9*%* metals basis) were procured. The palladium precursor was dissolved in 20 *ml* distilled water. After addition of the alumina support, the solvent was removed at 100 mbar, 60°C and a rotation speed of 90 rpm. Afterwards the impregnated pellets were calcined at 500*°C* in air for 3 *h* (2 $K\ min^{-1}$). The resulting pellets were then added to an aqueous zinc nitrate solution, dried in a rotational evaporator and calcined again at the same conditions as before. Finally, the catalyst was reduced in a 10 *vol.%* H_2 in N_2 flow at 440*°C* for 2 *h*.

Schematic setup of the laboratory plant

The plant used for the experiments of this study comprises reactant supplies for the gases dimethyl ether (DME, Air Liquide, purity 99.9 *wt.%*), Nitrogen (Air Liquide, purity 99.999 *vol.%*) and hydrogen (Air Liquide, purity 99.999 *vol.%*). The gases are fed into the reactor by the use of mass flow controllers (all Bronkhorst). The water supply consist of a 10 *L* canister, an HPLC pump, a cori-flow controller (Bronkhorst) and a total evaporator (ParTeQ). After the evaporator a vessel with a capacity of about 0.5 *L* is used to dampen pressure surges during evaporation. The reactants are mixed in line before entering the reactor. The catalyst is kept in a basket in the upper part of the reactor. A thermocouple in the catalyst bed is used for temperature control. The pressure in the reactor is maintained by an back pressure regulator (BPR). The effluent gas from the reactor is analysed with a Agilent 490 Micro GC after separation of water and methanol in a condenser. For the experiments with water-gas-shift catalyst a second reactor was added after the BPR. The SRD as well as the WGS reactor can be bypassed.

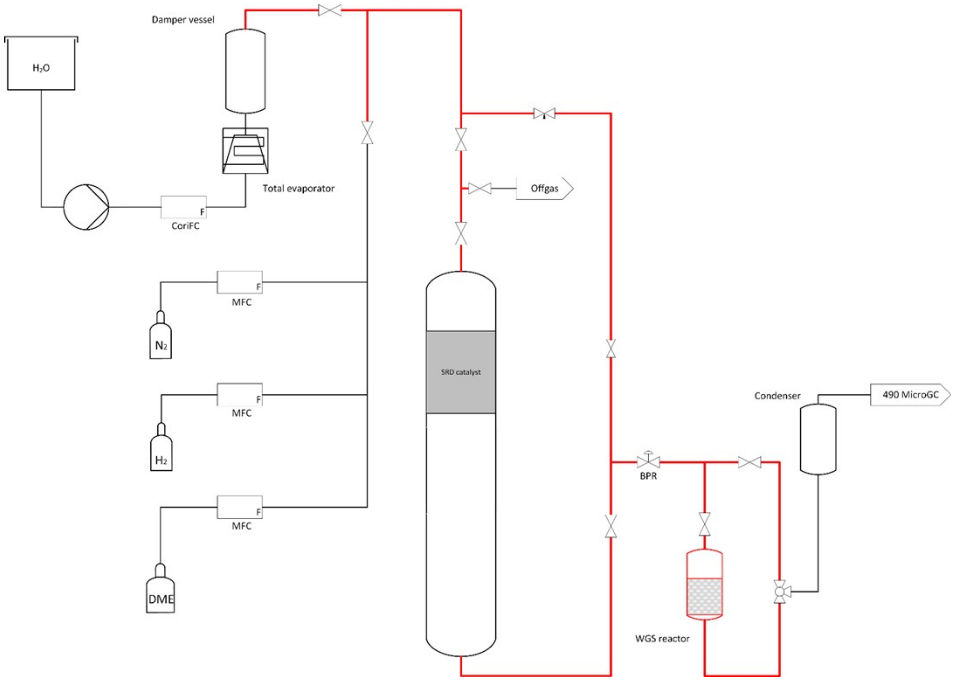

Figure S1: Setup of the laboratory plant used for the steam reforming of DME (SRD). A

Setup and method of the online GC

The Agilent 490 Micro GC is equipped with three channels consisting of a column and a TCD each. A measurement starts with 30 *s* sampling time, followed by a pre-separation over a 1 *m* PoraPlot Q precolumn and injection.

Table S1: Specification of the used setup and method of the Agilent 490 Micro GC

Channel Nr.	Column Type	T_{Column}/ °C	Backflush time/ s	Carrier Gas	Detected components in order of t_R
1	10m MS5A	70	9.0	Ar	He, H_2, O_2, N_2, CH_4, CO
2	10m PPQ	80	15.0	He	CH_4, CO_2, C_2H_4, C_2H_6, C_3H_6, C_3H_8/ C_4H_8, H_2O, MeOH, DME
3	6m 5CB-Sil	50	-	He	CO_2, H_2O, DME, MeOH

Results of the characterization of different metal oxide supports with N_2-physisorption and investigation of their MSR activity

Table S2: Investigation of the MSR activity of the metal oxides used for the support variation in combination with γ-Al_2O_3: DME conversion, selectivities ~~to C_1 products~~ and methane productivity after subtraction of the productivity of 3 *g* γ-Al_2O_3 (*p* = 2 bar_{abs}; *T* = 350°C; n_{H2O}:n_{DME}:n_{N2} = 5:1:1.5; $m_{support}$= 3 *g*;

Support	X_{DME} / %	$S_{CO2,g}$ ($S_{CO2,c}$) / %	$S_{CO,g}$ ($S_{CO,c}$)/ %	$S_{CH4,g}$ ($S_{CH4,c}$)/ %	$S_{MeOH,g}$ / %	P_{CH4} / $\mu mol_{CH4}\ g_{cat}^{-1}\ h^{-1}$
γ-Al_2O_3 + γ-Al_2O_3	33.4	0.1 (9.8)	0.4 (41.3)	0.4 (48.8)	99.1	56
γ-Al_2O_3 + SiO_2	32.1	0.1 (21.3)	0.2 (41.6)	0.2 (37.0)	99.5	1
γ-Al_2O_3 + TiO_2	33.1	0.1 (4.0)	0.8 (41.7)	1.1 (54.3)	98.0	264
γ-Al_2O_3 + ZrO_2	32.3	0.1 (12.6)	0.3 (53.5)	0.2 (33.9)	99.4	5

$m_{γ-Al2O3}$ = 3 g)

Table S3: Acidity and basicity determined by NH_3- and CO_2-TPD, s_{BET}, $v_{p,tot}$ and $\bar{d}_p$ of the pelletized metal oxide supports (pure and impregnated with 6 *wt.%* In_2O_3) determined by N_2-physisorption

	γ-Al_2O_3	In_2O_3/Al_2O_3	SiO_2	In_2O_3/SiO_2	TiO_2	In_2O_3/TiO_2	ZrO_2	In_2O_3/ZrO_2
Acidity / $mmol_{NH3}\ g^{-1}$	1.77	-	0.07	-	0.49	-	0.52	0.52
Basicity / $mmol_{CO2}\ g^{-1}$	2.27	-	0.09	-	1.21	-	0.54	0.38
s_{BET} / $m^2\ g^{-1}$	239	230	240	223	166	125	57	50
$v_{p,tot}$ / $cm^3\ g^{-1}$	0.78	0.72	0.99	0.91	0.46	0.36	0.24	0.19
$\bar{d}_p$ / nm	13	13	17	16	11	12	17	16

H_2-TPR of In_2O_3/ZrO_2

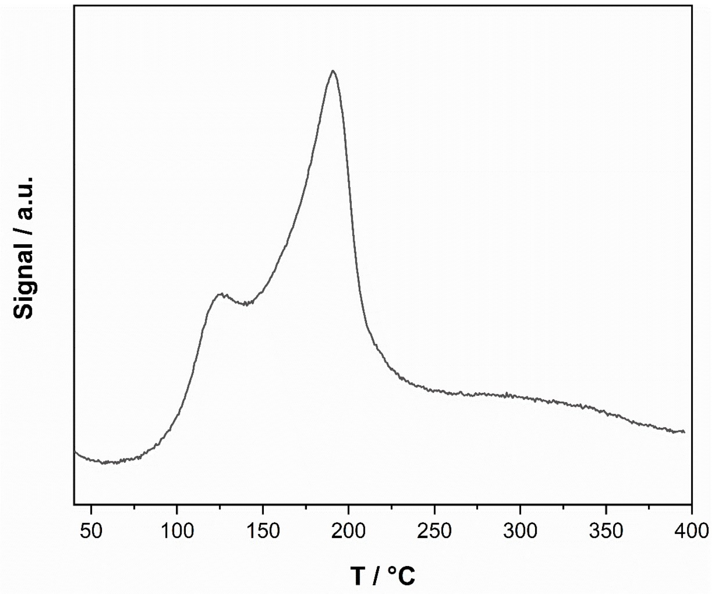

Figure S2: TPR profile of In_2O_3/ZrO_2 with 10.5 *wt.%* indium content

Comparison of the crystal phases of In_2O_3/ZrO_2 before and after reaction determined by X-ray diffraction

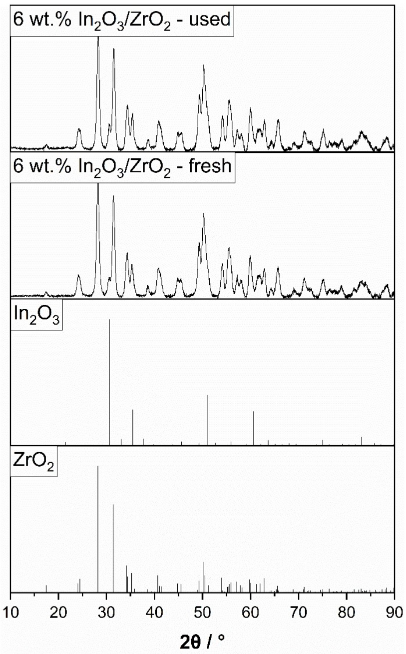

Figure S3: Comparison of the crystal phases of 6 *wt.%* In_2O_3/ZrO_2 catalyst as synthesized and after 48 *h* use in SRD (*p* = 2 bar_{abs}; *T* = 350°C; n_{H2O}:n_{DME}:n_{N2} = 5:1:1.5; $m_{MSR\text{-}Cat}$ = 3 *g*; $m_{\gamma\text{-}Al2O3}$ = 3 *g*

Additional experimental and analytical data complementing Figure 3 in the manuscript

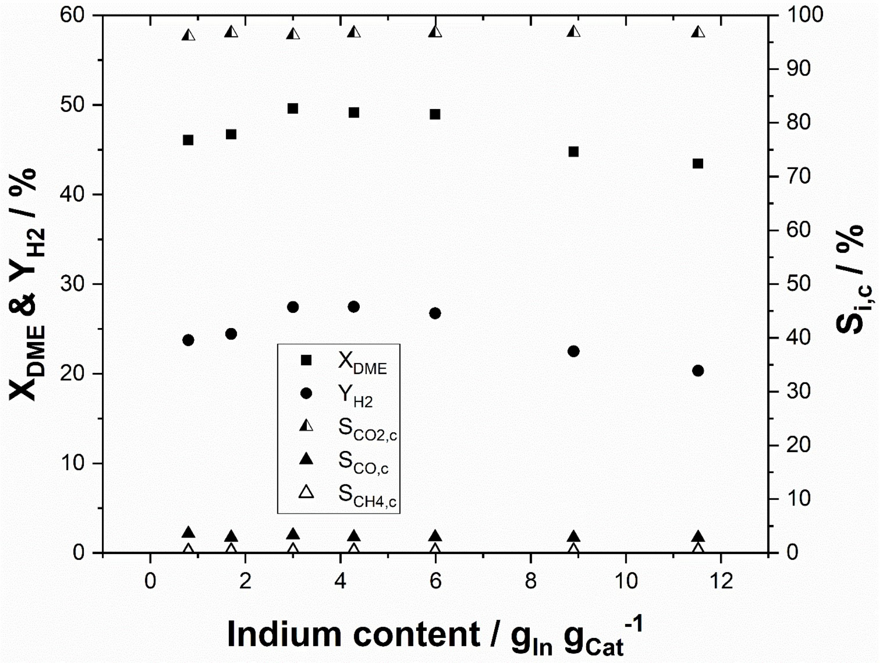

Figure S4: Conversions, H_2-yields and selectivities using In_2O_3/ZrO_2 catalysts with different indium content related to indium mass ($P_{H2,In}$) and total mass ($P_{H2.Cat}$) of the reforming catalyst (p = 2 *bar(a)*; T = 350 *°C*; molar ratio of n_{H2O}:n_{DME}:n_{N2} = 5:1:1.5; $m_{\gamma\text{-}Al2O3}$ = 3 *g*; $t_{reaction}$ = 18 *h*; *GHSV* = 2500 h^{-1})

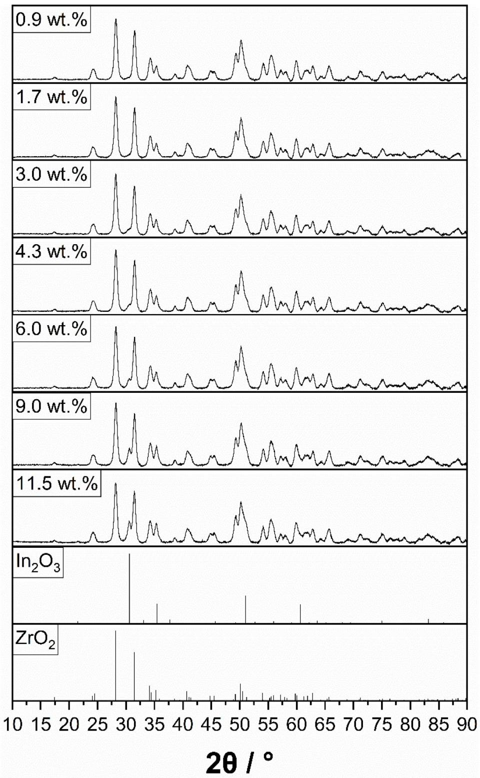

Figure S5: X-ray diffraction patterns of In_2O_3/ZrO_2 catalysts with different indium loadings used for the determination of the crystallite size depicted in Table S4; patterns of pure In_2O_3 (reference code: 98-016-9429) and ZrO_2 (reference code: 98-041-7639) derived from the HighScore Plus Database for reference.

After the diffraction patterns of the different In_2O_3/ZrO_2 catalysts were recorded, the data were analysed with Panalytical's HighScore Plus (V3.0.5). The baseline and peaks of the sample were determined. Afterwards the diffraction pattern was fitted and its reflexes deconvoluted with a pseudo-Voigt shape function. The average crystallite size (d_c) of In_2O_3 was estimated from the Scherrer equation with the (222) reflex located at 2θ = 30.6°:

$$d_c = \frac{k\lambda}{\beta cos\theta} \tag{S1}$$

where k represents the shape factor (0.89 assuming spherical particles), λ the wavelength of the Cu-Kα radiation (0.154 *nm*), β the Full Width at Half Maximum (FWHM) and θ the Bragg angle. For FWHM the value given by HighScore Plus in the peak list was used. Instrumental line broadening was neglected due to the absence of a suitable standard.

Table S4: Crystallite size of In_2O_3/ZrO_2 catalysts with different indium content calculated with the Scherrer equation from the characteristic reflex at 2θ = 30.6°.

Indium content / *wt.%*	Crystallite size d_c / *nm*
3.0	8.4
4.3	9.3
6.0	11.0
9.0	12.3
11.5	12.4

Results of N_2-physisorption of In_2O_3/ZrO_2 catalysts with different indium content

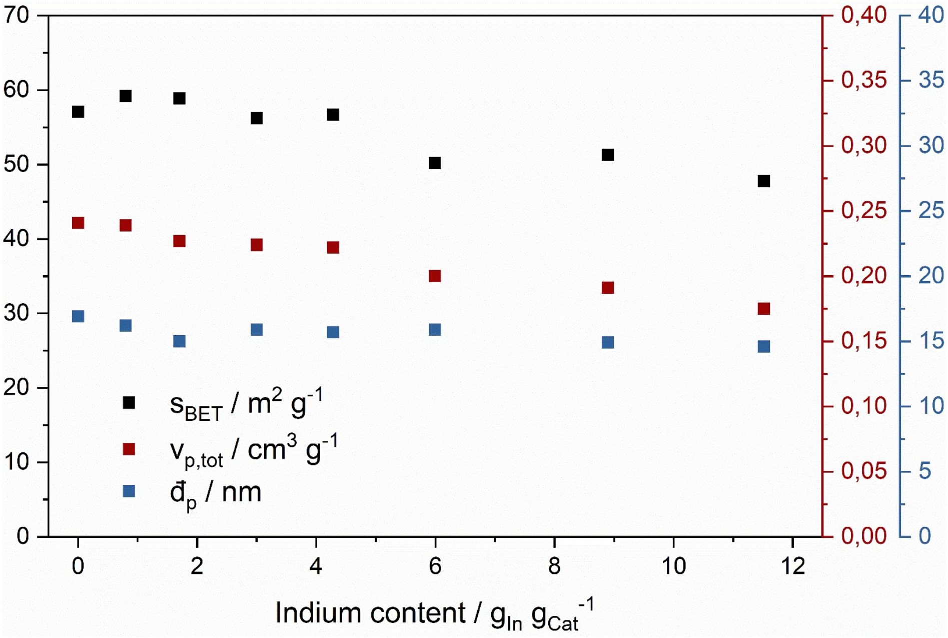

Figure S6: Specific surface area (s_{BET}), total pore volume ($v_{p,tot}$) and avarage pore diameter ($đ_p$) of In_2O_3/ZrO_2 catalysts with varied indium content.

Additional experimental data

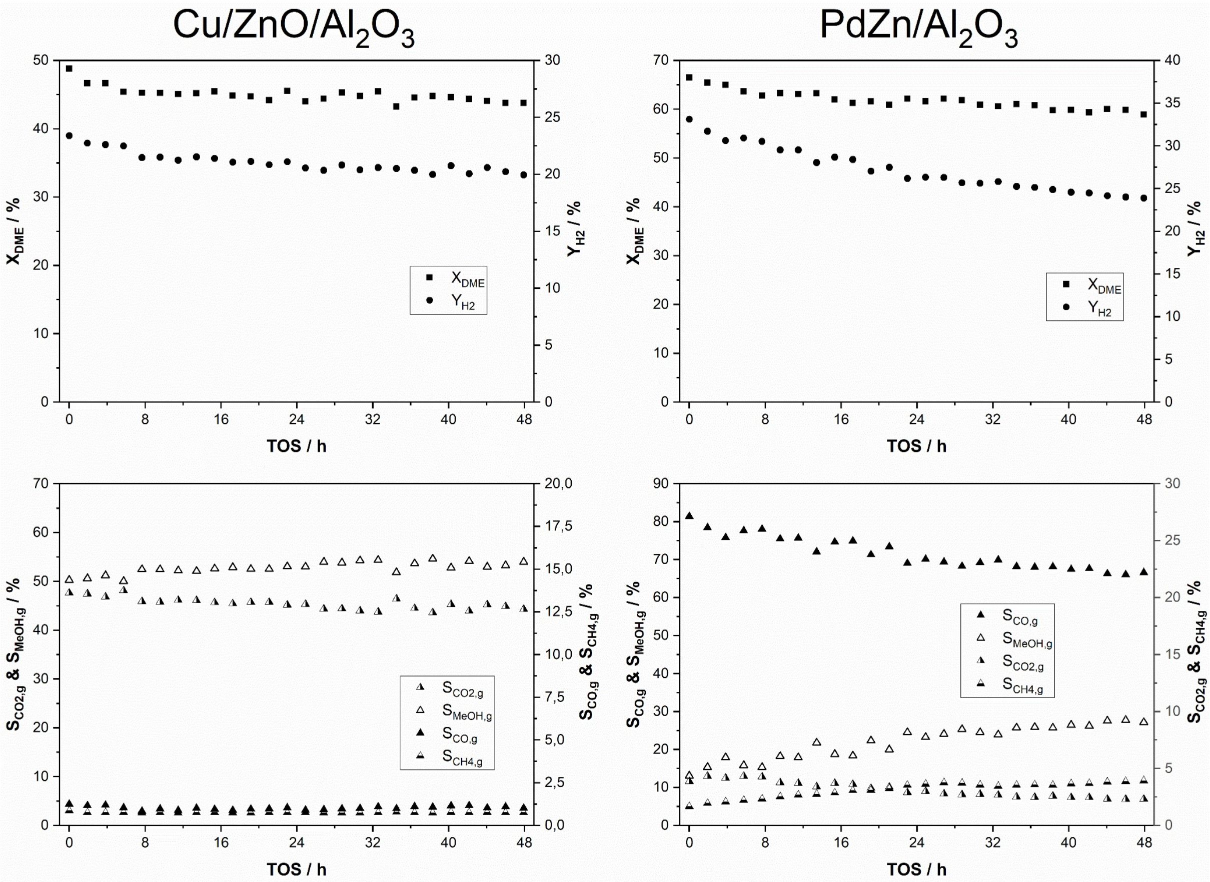

Figure S7: Stability of commercial Cu/ZnO/Al$_2$O$_3$ and a self synthesized 1 *wt.%* PdZn/Al$_2$O$_3$ catalyst compared based on DME conversion, hydrogen yield and selectitivity to methane, methanol, CO and CO$_2$ (p = 2 bar_{abs}; T = 350°C; n_{H2O}:n_{DME}:n_{N2} = 5:1:1.5; $m_{MSR\text{-}Cat}$ = 3 g; $m_{\gamma\text{-}Al2O3}$ = 3 g; $t_{reaction}$ = 48 h

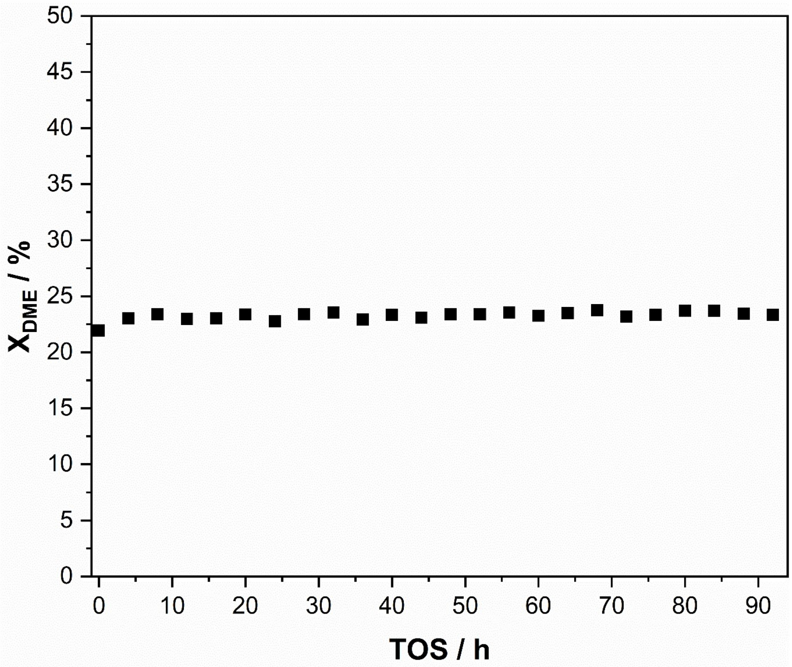

Figure S8: DME conversion of commercial γ-Al$_2$O$_3$ pellets over 90 *h* time on stream (p = 2 bar_{abs}; T = 400°C; n_{H2O}:n_{DME}:n_{N2} = 5:1:1.5; $m_{\gamma\text{-}Al2O3}$ = 0.25 g

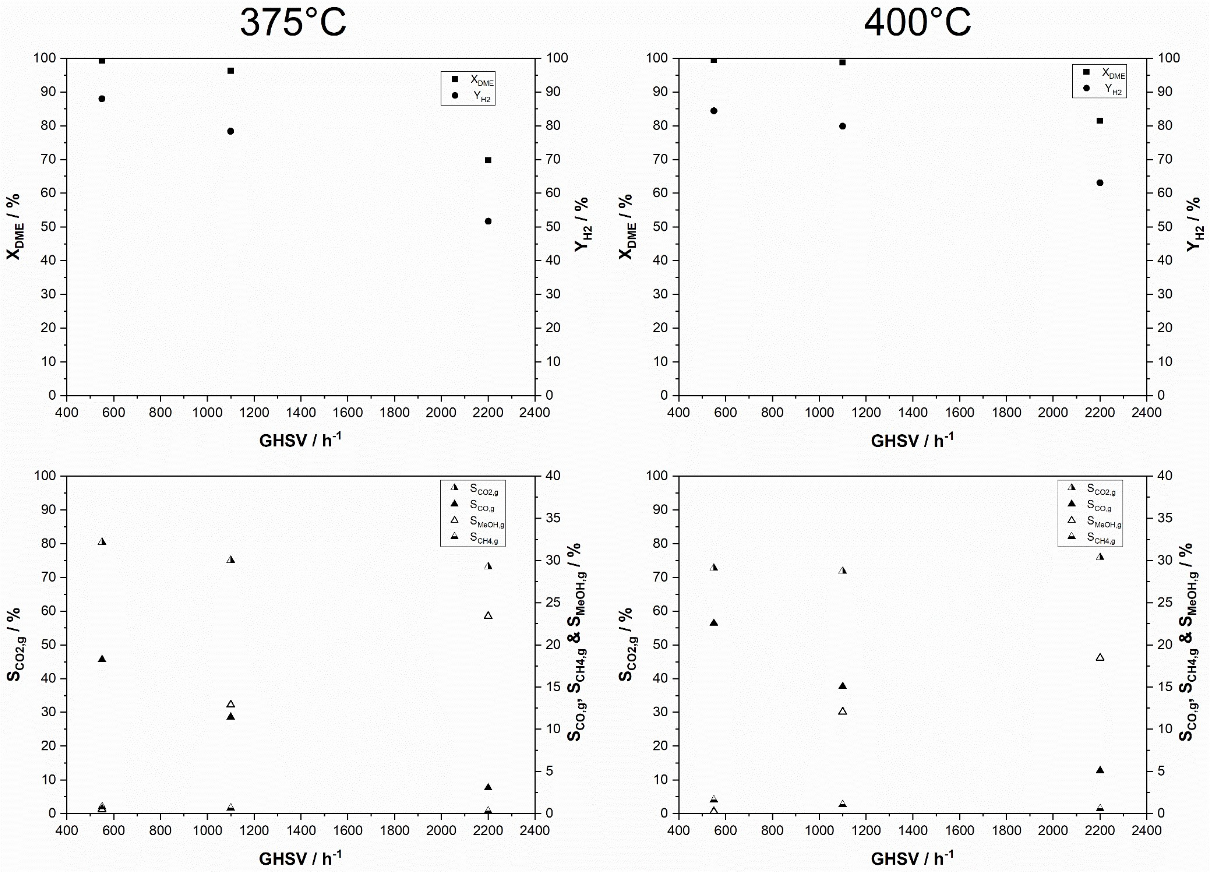

Figure S9: Effect of *GHSV* and process temperature on DME conversions, hydrogen yields and C_1 selectivities (p = 2 bar_{abs}; T = 375-400°*C*; n_{H2O}:n_{DME}:n_{N2} = 5:1:1.5; $m_{In2O3/ZrO2}$ = 36 *g* (3 *wt.%* indium content); $m_{\gamma\text{-}Al2O3}$ = 9 *g*

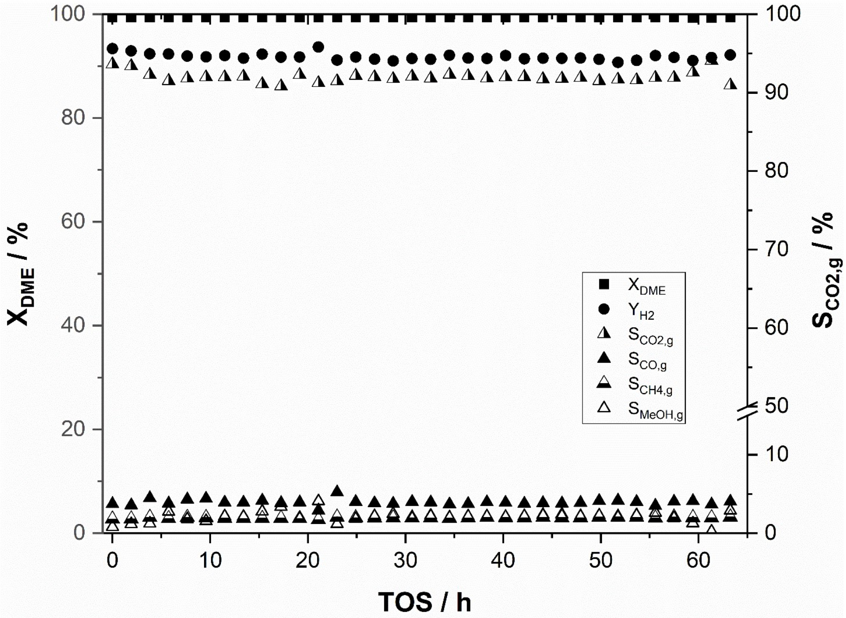

Figure S10: DME conversion, hydrogen yield and selectivity to C_1 products of the combined concept of SRD and WGS over 64 *h* time on stream (p = 2 bar_{abs}; T = 400°*C*; n_{H2O}:n_{DME}:n_{N2} = 5:1:1.5; $m_{In2O3/ZrO2}$ = 36 *g* (3.6 *wt.%* indium content); $m_{\gamma\text{-}Al2O3}$ = 9 *g*; $m_{ShiftMax\text{-}240}$ = 10 *g*, *GHSV* = 550 h^{-1}